

# Composition dependence of the specific heat of FeSi

Carolina Burger<sup>1\*</sup>, Andreas Bauer<sup>1,2</sup> and Christian Pfleiderer<sup>1,2,3</sup>

**1** Physik-Department, Technische Universität München, D-85748 Garching, Germany

**2** Zentrum für Quantum Engineering (ZQE), Technische Universität München, D-85748 Garching, Germany

**3** Munich Center for Quantum Science and Technology (MCQST), Technische Universität München, D-85748 Garching, Germany

\* carolina.burger@tum.de

February 1, 2023



*International Conference on Strongly Correlated Electron Systems  
(SCES 2022)*

*Amsterdam, 24-29 July 2022*

doi:[10.21468/SciPostPhysProc.?](https://doi.org/10.21468/SciPostPhysProc.)

## Abstract

Recently, a high-mobility surface conduction channel and in-gap states were identified in the correlated small-gap semiconductor FeSi using electrical transport measurements and high-resolution tunneling spectroscopy. The mobility of the charge carriers in the surface channel is quantitatively reminiscent of topological insulators, but displays a lack of sensitivity to the presence of ferromagnetic impurities as studied by means of a series of single crystals with slightly different starting compositions. Here, we report measurements of the specific heat of these crystals. At low temperatures, a shallow maximum is observed in the specific heat divided by temperature. This maximum is suppressed under magnetic field, characteristic of a Schottky anomaly associated with magnetic impurities. In comparison, the height of this maximum decreases with increasing initial iron content.

## 1 Introduction

FeSi is a correlated small-gap semiconductor in which an unusual temperature dependence of the electrical and magnetic properties has been attracting scientific interest for several decades [1–3]. As illustrated by means of the temperature dependence of the electrical resistivity shown in Fig. 1(a), FeSi exhibits a crossover around 200 K between a paramagnetic metal with strong spin fluctuations at high temperatures, denoted regime I, and a semiconducting state with reduced magnetic susceptibility featuring an energy gap of about 60 meV, denoted regime II [4–8]. For decreasing temperature, the resistivity continues to increase at a reduced slope below 100 K, denoted regime III, followed by a saturation on logarithmic scales at low temperatures, denoted regime IV [9, 10]. The magnetic susceptibility increases by about two orders of magnitude in regimes III and IV [11]. While band structure calculations established unambiguously that FeSi is a band insulator at low temperatures [12–14], the unusual metallization and paramagnetism at high temperatures was attributed to correlation-induced incoherence under increasing temperature [15]. The saturation of the resistivity at low temperatures was attributed to the emergence of an impurity band, with ferromagnetic impurities potentially adding to the complexity of the low-temperature properties [16–18].

31 Recently, the emergence of a high-mobility surface conduction channel at low tempera-  
 32 tures was inferred from the electrical transport properties of a series of single crystals of FeSi  
 33 prepared under systematic variation of the initial iron content using the optical floating-zone  
 34 technique [19–23]. This observation was corroborated by means of measurements on thin needles  
 35 grown from tin flux [24] as well as high-resolution tunneling spectroscopy that revealed  
 36 two in-gap states in the low-temperature regime of the samples grown by the floating-zone  
 37 technique [25]. The surface-to-bulk ratios of the charge carrier densities and mobilities ob-  
 38 served in the transport properties compare quantitatively with values observed in topological  
 39 insulators such as  $\text{Bi}_2\text{Te}_3$  [19, 20, 26]. Most notably, the surface channel in FeSi appears to  
 40 exhibit a remarkable robustness against the presence of ferromagnetic impurities. An open  
 41 question concerns, in turn, whether this robustness represents a hallmark of FeSi that is also  
 42 reflected in bulk properties.

## 43 2 Experimental Methods

44 In this paper, we report a study of the specific heat of the same series of single crystals studied  
 45 in Refs. [19, 20], as prepared by means of the optical floating-zone technique using slightly  
 46 different starting compositions  $\text{Fe}_{1+x}\text{Si}$  [21–23]. The magnetization and electrical transport  
 47 properties of these single crystals were reported in Refs. [19, 20, 25]. In addition, a single  
 48 crystal with an iron deficiency  $x = -0.005$  was studied. Samples cut from the start of the  
 49 single-crystal growth process (close to the initial grain selection) and from the end (close to  
 50 the final quenched zone) were investigated as summarized in Tab. 1. Consistent with the de-  
 51 tection limits of standard techniques for metallurgical characterization, such as powder x-ray  
 52 diffraction or energy-dispersive x-ray spectroscopy, and the tiny variation of the starting com-  
 53 positions, no systematic variations of the composition of the samples after the growth process  
 54 were resolved using these methods. In comparison, studies of the density and nature of struc-  
 55 tural point defects using techniques such as positron annihilation spectroscopy, planned for  
 56 the future, may provide valuable insights, as demonstrated on isostructural  $\text{Mn}_{1+x}\text{Si}$  [27, 28].  
 57 Such studies, however, were well beyond the scope of the work presented in this manuscript.

Sample	Starting composition	Location in float-zoned ingot
A1	$\text{Fe}_{0.99}\text{Si}$	start
A2	$\text{Fe}_{0.99}\text{Si}$	end
AB	$\text{Fe}_{0.995}\text{Si}$	start
B1	FeSi	start
B2	FeSi	end
C	$\text{Fe}_{1.01}\text{Si}$	start

Table 1: Overview of the samples studied in this paper (see also Refs. [19, 20, 25]). For each sample, the chemical composition of the polycrystalline rods before float-zoning and the location from which the sample was cut within the float-zoned single-crystal ingot are stated.

58 For the present study, cubes with an edge length of 1 mm were prepared, each with two  
 59 surfaces perpendicular to  $\langle 100 \rangle$  and four surfaces perpendicular to  $\langle 110 \rangle$ . The specific heat  
 60 measurements were carried out in a Quantum Design physical property measurement system  
 61 at temperatures down to 1.9 K and under magnetic fields up to 14 T. The single crystal cubes  
 62 were mounted on the platform of the measurement puck by means of a tiny amount of Apiezon

63 N grease. Prior to mounting each sample, the heat capacity of the grease was measured in  
 64 order to subtract it from the total heat capacity. Precise subtraction proved to be crucial for  
 65 the determination of the heat capacity of the  $\text{Fe}_{1+x}\text{Si}$  samples<sup>1</sup>. All measurements were carried  
 66 out using a quasi-adiabatic large heat pulse technique, in which heat pulses had a size of 30% of  
 67 the temperature at the start of the pulse [29]. For each specific heat curve, data were measured  
 68 at 80 starting temperatures in a logarithmic spacing, covering the temperature regime from  
 69 1.9 K to 270 K. The heat pulses and concomitant data collection were repeated three times at  
 70 each temperature.

### 71 3 Experimental Results

72 A typical temperature dependence of the specific heat of FeSi is shown in Fig. 1(b), for the case  
 73 of sample A1. Both the resistivity shown in Fig. 1(a) and the specific heat shown in Fig. 1(b)  
 74 were measured on samples cut from the same location of the same ingot, referred to as samples  
 75 A1r and A1, respectively. The specific heat as a function of temperature is characteristic of a  
 76 nonmagnetic crystal in which phonon contributions dominate. It approaches the Dulong–  
 77 Petit value of  $6R = 49.9 \text{ J mol}^{-1}\text{K}^{-1}$  at high temperatures. No anomalies suggestive of phase  
 78 transitions were observed in any of the samples in the temperature and field range investigated.

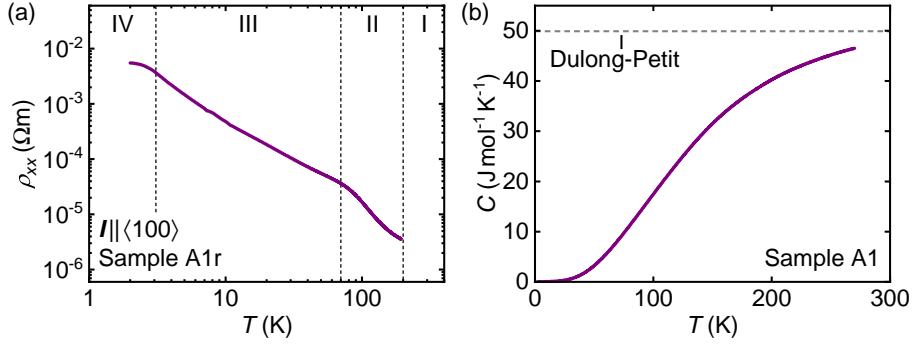


Figure 1: Temperature dependence of the low-temperature properties of FeSi for samples A1r and A1 in zero magnetic field. (a) Electrical resistivity for current along  $\langle 100 \rangle$  on a double-logarithmic scale. Four regimes may be distinguished as a function of temperature, denoted I through IV; see text for details. Data taken from Refs. [19, 20]. (b) Specific heat. No anomalies suggestive of phase transitions are observed in the temperature range studied.

79 For the analysis of our data, we consider the specific heat divided by temperature,  $C/T$ , as  
 80 illustrated for sample A1 in Fig. 2(a). A prominent feature concerns a shallow maximum below  
 81  $\sim 10$  K, consistent with Ref. [16], where the maximum was attributed to a Schottky anomaly.  
 82 In Ref. [16], an additional maximum was reported in the specific heat at temperatures well  
 83 below 2 K, i.e., below the temperature range investigated in our study. To fit our data we  
 84 use the empirical description suggested in Ref. [16], however, taking into account a single  
 85 Schottky anomaly only. Beyond the conventional terms proportional to  $T$  and  $T^3$ , an additional  
 86 contribution proportional to  $T^5$  as well as the Schottky anomaly were included, resulting in

$$C = \gamma T + \beta T^3 + \delta T^5 + a_1 \frac{(T_1/T)^2 \exp(T_1/T)}{[1 + \exp(T_1/T)]^2}. \quad (1)$$

<sup>1</sup>As part of the studies reported here, we noticed that the specific heat presented in the supplemental material of Ref. [25] is dominated by contributions of the grease and hence erroneous. An erratum will be published separately.

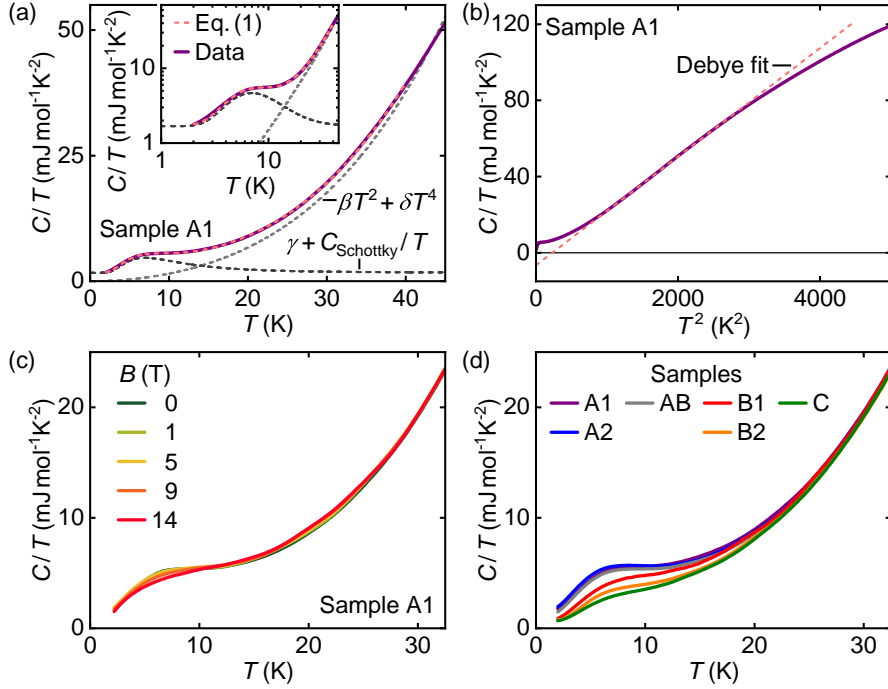


Figure 2: Specific heat divided by temperature as function of temperature. (a) Data of sample A1 in zero magnetic field. At low temperatures, a shallow maximum is observed that is suggestive of a Schottky anomaly. The dashed red line corresponds to a fit according to Eq. (1). The dashed dark and light gray lines correspond to the sum of the terms dominating at low and high temperatures, respectively. Inset: Data on a double-logarithmic scale. (b) Specific heat divided by temperature as a function of temperature squared. The dashed line represents a linear regression corresponding to a phonon contribution as expected in a Debye model. See text for details. (c) Specific heat divided by temperature of sample A1 under selected magnetic fields up to 14 T. With increasing field, the maximum suggestive of a Schottky anomaly is suppressed. (d) Zero-field data for samples with different initial compositions. At temperatures above  $\sim 20$  K, the data essentially track each other. At low temperatures, the height of the maximum decreases with increasing iron content in the starting composition prior to crystal growth.

87 When fitting the coefficients  $\gamma$ ,  $\beta$ ,  $\delta$ , and  $a_1$  as well as the Schottky temperature  $T_1$  for sample  
 88 A1, the following values are obtained, as summarized in Tab. 2:  $\gamma_{\text{A1}} = 1.68 \text{ mJ mol}^{-1} \text{K}^{-2}$ ,  
 89  $\beta_{\text{A1}} = 1.45 \cdot 10^{-2} \text{ mJ mol}^{-1} \text{K}^{-4}$ ,  $\delta_{\text{A1}} = 5.67 \cdot 10^{-6} \text{ mJ mol}^{-1} \text{K}^{-6}$ ,  $a_{1,\text{A1}} = 54.3 \text{ mJ mol}^{-1} \text{K}^{-1}$ ,  
 90 and  $T_{1,\text{A1}} = 22.5 \text{ K}$ . The corresponding fit is shown as a dashed red line in Fig. 2(a). The  
 91 value of  $\beta_{\text{A1}}$  corresponds to a Debye temperature  $\Theta_{\text{D,A1}} = 645 \text{ K}$ . It may be helpful to note  
 92 that when fitting the data without the contribution proportional to  $T^5$ , values of  $\gamma$  are negative  
 93 and thus not physical. This observation is illustrated in Fig. 2(b) showing a linear fit of  $C/T$  as  
 94 a function of  $T^2$ , where the axis intercept corresponds to  $\gamma$  and the slope to  $\beta$ . The values of  
 95  $\beta$  inferred without the  $T^5$  contribution translate to Debye temperatures of the order of 500 K,  
 96 consistent with values reported for other isostructural transition-metal compounds for which  
 97 the data were analyzed without  $T^5$  terms as well [30,31].

98 Integration of the term describing the Schottky anomaly yields an estimate for the underlying  
 99 entropy. For sample A1, we obtain  $\Delta S_{1,\text{A1}} = 37.3 \text{ mJ mol}^{-1} \text{K}^{-1} \approx 0.006 R \ln 2$ , correspond-  
 100 ing to about 0.006 two-level centers per formula unit of FeSi. As no data were measured below  
 101 2 K in our study, we cannot exclude the putative presence of a second Schottky anomaly at

102 very low temperatures previously reported in Ref. [16]. Fitting our data, we estimate that such  
 103 an anomaly may yield an entropy not larger than  $\Delta S_{2,A1} < 0.002 R \ln 2$ . This concentration  
 104 suggests that the two-level centers are located in the bulk of the material. For comparison,  
 105 when assuming that the two-level centers emerge at the surface of the sample and that each  
 106 formula unit may support a single two-level center, a surface layer of a thickness of  $\sim 1 \mu\text{m}$   
 107 would be required, i.e., much thicker than typically observed for surface-induced phenomena.

108 It is instructive to note that, in contrast to the specimens investigated in our study, the sam-  
 109 ples studied in Ref. [16] were grown from vapor transport. Various materials properties, such  
 110 as the magnetization and the Hall effect reported in Ref. [16], as well as tests we performed  
 111 ourselves on samples of FeSi grown from vapor transport consistently suggest that such sam-  
 112 ples may contain substantial concentrations of magnetic impurities, such as elemental iron. In  
 113 turn, when comparing our results to those reported in Ref. [16], namely  $\gamma_p = 1.1 \text{ mJ mol}^{-1}\text{K}^{-2}$ ,  
 114  $\beta_p = 0.91 \cdot 10^{-2} \text{ mJ mol}^{-1}\text{K}^{-4}$ ,  $\delta_p = 11 \cdot 10^{-6} \text{ mJ mol}^{-1}\text{K}^{-6}$ ,  $a_{1,p} = 9.2 \text{ mJ mol}^{-1}\text{K}^{-1}$ ,  $T_{1,p} =$   
 115  $6.8 \text{ K}$ ,  $a_{2,p} = 11 \text{ mJ mol}^{-1}\text{K}^{-1}$ ,  $T_{2,p} = 0.95 \text{ K}$ ,  $\Delta S_{1,p} = 6.3 \text{ mJ mol}^{-1}\text{K}^{-1}$ , and  $\Delta S_{2,p} =$   
 116  $7.9 \text{ mJ mol}^{-1}\text{K}^{-1}$ , two key differences become apparent. First, compared to our results,  $\beta$   
 117 is smaller by a factor of 1.6 while  $\delta$  is larger by a factor of 2. In a fit using Eq. (1), these  
 118 two parameters are connected, where smaller values of  $\beta$  result in larger values of  $\delta$  and vice  
 119 versa. Since in Ref. [16] specific heat data were measured down to temperatures as low as  
 120 60 mK and presented on a double-logarithmic scale up to 35 K, the behavior at high temper-  
 121 atures may have been accounted for less accurately. Note that  $\beta_p = 0.91 \cdot 10^{-2} \text{ mJ mol}^{-1}\text{K}^{-4}$   
 122 corresponds to a Debye temperature  $\Theta_{D,p}^* = 753 \text{ K}$  instead of the value  $\Theta_{D,p} = 377 \text{ K}$  stated in  
 123 Ref. [16]. Second, the Schottky anomaly at  $T_1$  is smaller and shifted to lower temperatures.  
 124 As discussed below, this anomaly is sensitive to the detailed composition of the sample, where  
 125 the values reported in Ref. [16] are consistent with a large iron content.

126 As illustrated in Fig. 2(c), under magnetic fields up to 14 T, the maximum at  $T_1$  observed  
 127 in our samples decreases in height and the associated entropy release shifts to higher tempera-  
 128 tures. Such a field dependence suggests qualitatively that the maximum is linked to magnetic  
 129 degrees of freedom, consistent, for instance, with magnetic impurities.

130 Comparing the specific heat of different samples, as shown in Fig. 2(d) in terms of  $C/T$  in  
 131 zero magnetic field, several characteristics appear to be the same for all compositions. First,  
 132 at temperatures above  $\sim 20 \text{ K}$  data for all samples studied track each other, indicating essen-  
 133 tially identical contributions due to phonons at high temperatures. This finding suggests that  
 134 the small variations of the starting composition do not affect the crystal structure on a funda-  
 135 mental level. Second, all samples exhibit a shallow maximum at low temperatures, suggestive  
 136 of a Schottky anomaly as discussed above. The height of this anomaly varies systematically  
 137 between samples. Third, for all samples studied, the specific heat is in excellent agreement  
 138 with Eq. (1). The coefficients inferred from these fits are summarized in Tab. 2. Fourth, in  
 139 all samples studied, the specific heat at high temperatures is insensitive to applied magnetic  
 140 fields up to 14 T (not shown).

141 The change in height of the Schottky anomaly at  $T_1$  represents the most prominent dif-  
 142 ference between samples. As reflected in the evolution of the parameter  $a_1$  and the entropy  
 143 release  $\Delta S_1$ , the size of the anomaly and therefore the number of two-level centers per formula  
 144 unit decreases with increasing iron content. This decrease contradicts the expectation that an  
 145 increase of the iron content leads to an increase of the density of magnetic impurities and  
 146 hence two-level centers. Instead, the opposite evolution appears to take place in the specific  
 147 heat of the samples of FeSi in our study. Such a counter-intuitive behavior, in combination with  
 148 the field dependence of the maximum, which is suggestive of a magnetic origin, indicates that  
 149 the Schottky anomaly may not be readily connected with a two-level energy scheme arising  
 150 from single iron impurities only. Adding a further aspect, the characteristic temperature  $T_1$  re-  
 151 mains essentially unchanged under increasing iron content, i.e., it does not appear to scale in

Sample	$\gamma$ [mJ mol <sup>-1</sup> K <sup>-2</sup> ]	$\beta$ [10 <sup>-2</sup> mJ mol <sup>-1</sup> K <sup>-4</sup> ]	$\delta$ [10 <sup>-6</sup> mJ mol <sup>-1</sup> K <sup>-6</sup> ]	$a_1$ [mJ mol <sup>-1</sup> K <sup>-1</sup> ]	$T_1$ [K]	$\Theta_D$ [K]	$\Delta S_1$ [mJ mol <sup>-1</sup> K <sup>-1</sup> ]
A1	1.68	1.45	5.67	54.3	22.5	645	37.3
A2	1.72	1.39	6.02	55.4	21.1	654	38.1
AB	1.39	1.42	5.88	55.9	21.9	649	38.4
B1	0.90	1.58	5.11	50.3	24.2	627	34.5
B2	0.59	1.57	5.27	40.1	23.6	628	27.5
C	0.57	1.57	5.28	30.4	24.0	628	20.9

Table 2: Overview of key parameters inferred from the specific heat of FeSi for the samples investigated in our study. For each sample, the coefficients  $\gamma$ ,  $\beta$ , and  $\delta$  are shown together with the coefficient  $a_1$  and the characteristic temperature  $T_1$  describing the Schottky anomaly at low temperatures. In addition, the Debye temperature  $\Theta_D$  calculated from the coefficient  $\beta$  and an estimate of the entropy  $\Delta S_1$  associated with the Schottky anomaly are presented.

152 an obvious way with the initial starting composition. This behavior contrasts the characteristic  
153 temperature of the onset of the saturation of the resistivity in regime IV [19, 20, 25].

154 In view of the sample dependence of the specific heat reported in this study, the lack of  
155 an anomaly in specific heat measurements carried out on thin needles grown from tin flux  
156 reported in Ref. [24] suggests substantial iron excess. Similarly, as discussed above, the rela-  
157 tively small anomaly reported for samples grown from vapor transport is consistent with iron  
158 excess, reflected also in the magnetization and Hall effect [16]. Taken together, these results  
159 motivate further studies on the interplay of impurities with the bulk and transport properties  
160 in FeSi, made possible by the optical floating-zone technique and the precise control of the  
161 starting compositions associated with it [23].

## 162 4 Conclusions

163 The specific heat of the correlated small-gap semiconductor FeSi was studied for a series of  
164 single crystals prepared from slightly different starting compositions [19, 20]. All samples  
165 studied exhibit a shallow maximum in  $C/T$  between 2 K and 10 K, reminiscent of a Schottky  
166 anomaly. Under magnetic field, this anomaly decreases in size, suggestive of a magnetic origin.  
167 However, as a function of increasing initial iron content, implying an increase of the density  
168 of magnetic impurities as observed in the magnetization, the height of the anomaly decreases.  
169 Further studies are needed to clarify if and in which way the specific heat at low temperature  
170 may be related to the robust high-mobility surface conduction channel [19, 20, 24].

## 171 Acknowledgements

172 We wish to thank A. Engelhardt and S. Mayr for fruitful discussions and assistance with the  
173 experiments. We also wish to thank the anonymous referee for pointing out the importance of  
174 the specific heat contribution of Apiezon N grease for our analysis.

175 **Funding information** This study has been funded by the Deutsche Forschungsgemeinschaft  
176 (DFG, German Research Foundation) under TRR80 (From Electronic Correlations to Func-  
177 tionality, Project No. 107745057, Project E1), SPP2137 (Skyrmionics, Project No. 403191981,  
178 Grant PF393/19), and the excellence cluster MCQST under Germany's Excellence Strategy  
179 EXC-2111 (Project No. 390814868). Financial support by the European Research Council

180 (ERC) through Advanced Grant and No. 788031 (ExQuiSid) is gratefully acknowledged.

## 181 References

- 182 [1] G. K. Wertheim, V. Jaccarino, J. H. Wernick, J. A. Seitchik, H. J. Williams and R. C. Sher-  
183 wood, *Unusual electronic properties of FeSi*, Phys. Lett. **18**, 89 (1965), doi:[10.1016/0031-](https://doi.org/10.1016/0031-9163(65)90658-X)  
184 [9163\(65\)90658-X](https://doi.org/10.1016/0031-9163(65)90658-X).
- 185 [2] M. Arita, K. Shimada, Y. Takeda, M. Nakatake, H. Namatame, M. Taniguchi, H. Negishi,  
186 T. Oguchi, T. Saitoh, A. Fujimori and T. Kanomata, *Angle-resolved photoemission*  
187 *study of the strongly correlated semiconductor FeSi*, Phys. Rev. B **77**, 205117 (2008),  
188 doi:[10.1103/PhysRevB.77.205117](https://doi.org/10.1103/PhysRevB.77.205117).
- 189 [3] M. Klein, D. Zur, D. Menzel, J. Schoenes, K. Doll, J. Röder and F. Reinert, *Evi-*  
190 *dence for itineracy in the anticipated Kondo insulator FeSi: A quantitative deter-*  
191 *mination of the band renormalization*, Phys. Rev. Lett. **101**, 046406 (2008),  
192 doi:[10.1103/PhysRevLett.101.046406](https://doi.org/10.1103/PhysRevLett.101.046406).
- 193 [4] V. Jaccarino, G. K. Wertheim, J. H. Wernick, L. R. Walker and S. Araj, *Paramagnetic*  
194 *excited state of FeSi*, Phys. Rev. **160**, 476 (1967), doi:[10.1103/PhysRev.160.476](https://doi.org/10.1103/PhysRev.160.476).
- 195 [5] S. Takagi, H. Yasuoka, S. Ogawa and J. H. Wernick, *<sup>29</sup>Si NMR studies of an “unusual”*  
196 *paramagnet FeSi: Anderson localized state model*, J. Phys. Soc. Jpn. **50**, 2539 (1981),  
197 doi:[10.1143/JPSJ.50.2539](https://doi.org/10.1143/JPSJ.50.2539).
- 198 [6] M. B. Hunt, M. A. Chernikov, E. Felder, H. R. Ott, Z. Fisk and P. Canfield, *Low-temperature*  
199 *magnetic, thermal, and transport properties of FeSi*, Phys. Rev. B **50**, 14933 (1994),  
200 doi:[10.1103/PhysRevB.50.14933](https://doi.org/10.1103/PhysRevB.50.14933).
- 201 [7] J. F. DiTusa, K. Friemelt, E. Bucher, G. Aeppli and A. P. Ramirez, *Metal–insulator transi-*  
202 *tions in the Kondo insulator FeSi and classic semiconductors are similar*, Phys. Rev. Lett.  
203 **78**, 2831 (1997), doi:[10.1103/PhysRevLett.78.2831](https://doi.org/10.1103/PhysRevLett.78.2831).
- 204 [8] P. S. Riseborough, *Heavy fermion semiconductors*, Adv. Phys. **49**, 257 (2000),  
205 doi:[10.1080/000187300243345](https://doi.org/10.1080/000187300243345).
- 206 [9] P. Lunkenheimer, G. Knebel, R. Viana and A. Loidl, *Hopping conductivity in FeSi*, Solid  
207 State Commun. **93**, 891 (1995), doi:[10.1016/0038-1098\(94\)00895-7](https://doi.org/10.1016/0038-1098(94)00895-7).
- 208 [10] L. Degiorgi, M. Hunt, H. R. Ott and Z. Fisk, *Transport and optical properties of FeSi*,  
209 Physica B **206–207**, 810 (1995), doi:[10.1016/0921-4526\(94\)00592-J](https://doi.org/10.1016/0921-4526(94)00592-J).
- 210 [11] Z. Schlesinger, Z. Fisk, H.-T. Zhang, M. B. Maple, J. DiTusa and G. Aeppli, *Un-*  
211 *conventional charge gap formation in FeSi*, Phys. Rev. Lett. **71**, 1748 (1993),  
212 doi:[10.1103/PhysRevLett.71.1748](https://doi.org/10.1103/PhysRevLett.71.1748).
- 213 [12] L. F. Mattheiss and D. R. Hamann, *Band structure and semiconducting properties of FeSi*,  
214 Phys. Rev. B **47**, 13114 (1993), doi:[10.1103/PhysRevB.47.13114](https://doi.org/10.1103/PhysRevB.47.13114).
- 215 [13] T. Jarlborg, *Electronic structure and properties of pure and doped  $\epsilon$ -FeSi from ab initio*  
216 *local-density theory*, Phys. Rev. B **59**, 15002 (1999), doi:[10.1103/PhysRevB.59.15002](https://doi.org/10.1103/PhysRevB.59.15002).
- 217 [14] J. Kuneš and V. I. Anisimov, *Temperature-dependent correlations in covalent insu-*  
218 *lators: Dynamical mean-field approximation*, Phys. Rev. B **78**, 033109 (2008),  
219 doi:[10.1103/PhysRevB.78.033109](https://doi.org/10.1103/PhysRevB.78.033109).

- 220 [15] J. M. Tomczak, K. Haule and G. Kotliar, *Signatures of electronic correlations in iron silicide*,  
221 Proc. Natl. Acad. Sci. USA **109**, 3243 (2012), doi:[10.1073/pnas.1118371109](https://doi.org/10.1073/pnas.1118371109).
- 222 [16] S. Paschen, E. Felder, M. A. Chernikov, L. Degiorgi, H. Schwer, H. R. Ott, D. P. Young, J. L.  
223 Sarrao and Z. Fisk, *Low-temperature transport, thermodynamic, and optical properties of*  
224 *FeSi*, Phys. Rev. B **56**, 12916 (1997), doi:[10.1103/PhysRevB.56.12916](https://doi.org/10.1103/PhysRevB.56.12916).
- 225 [17] N. E. Sluchanko, V. V. Glushkov, S. V. Demishev, M. V. Kondrin, V. Y. Ivanov, K. M. Petukhov,  
226 N. A. Samarin, A. A. Menovsky and V. V. Moshchalkov, *Ground state formation in a strong*  
227 *Hubbard correlation regime in iron monosilicide*, J. Exp. Theor. Phys. **92**, 312 (2001),  
228 doi:[10.1134/1.1354689](https://doi.org/10.1134/1.1354689).
- 229 [18] N. E. Sluchanko, V. V. Glushkov, S. V. Demishev, A. A. Menovsky, L. Weckhuysen and V. V.  
230 Moshchalkov, *Crossover in magnetic properties of FeSi*, Phys. Rev. B **65**, 064404 (2002),  
231 doi:[10.1103/PhysRevB.65.064404](https://doi.org/10.1103/PhysRevB.65.064404).
- 232 [19] M. Wagner, *Suche nach topologisch nichttrivialen Eigenschaften stark korrelierter Materi-*  
233 *alien*, Ph.D. thesis, Technische Universität München (2014).
- 234 [20] M. Wagner, R. Kortner, A. Bauer and C. Pfleiderer, *Emergence of high-mobility surface*  
235 *conduction in FeSi at low temperatures*, unpublished (2017).
- 236 [21] A. Neubauer, J. Bœuf, A. Bauer, B. Russ, H. v. Löhneysen and C. Pfleiderer, *Ultra-*  
237 *high vacuum compatible image furnace*, Rev. Sci. Instrum. **82**, 013902 (2011),  
238 doi:[10.1063/1.3523056](https://doi.org/10.1063/1.3523056).
- 239 [22] A. Bauer, G. Benka, A. Regnat, C. Franz and C. Pfleiderer, *Ultra-high vacuum compatible*  
240 *preparation chain for intermetallic compounds*, Rev. Sci. Instrum. **87**, 113902 (2016),  
241 doi:[10.1063/1.4967011](https://doi.org/10.1063/1.4967011).
- 242 [23] A. Bauer, G. Benka, A. Neubauer, A. Regnat, A. Engelhardt, C. Resch, S. Wurmehl, C. G. F.  
243 Blum, T. Adams, A. Chacon, R. Jungwirth, R. Georgii *et al.*, *Compositional studies of metals*  
244 *with complex order by means of the optical floating-zone technique*, Phys. Status Solidi B  
245 **259**, 2100159 (2022), doi:[10.1002/pssb.202100159](https://doi.org/10.1002/pssb.202100159).
- 246 [24] Y. Fang, S. Ran, W. Xie, S. Wang, Y. S. Meng and M. B. Maple, *Evidence for a conducting*  
247 *surface ground state in high-quality single crystalline FeSi*, Proc. Natl. Acad. Sci. USA **115**,  
248 8558 (2018), doi:[10.1073/pnas.1806910115](https://doi.org/10.1073/pnas.1806910115).
- 249 [25] B. Yang, M. Uphoff, Y.-Q. Zhang, J. Reichert, A. P. Seitsonen, A. Bauer, C. Pfleiderer  
250 and J. V. Barth, *Atomistic investigation of surface characteristics and electronic features*  
251 *at high-purity FeSi(110) presenting interfacial metallicity*, Proc. Natl. Acad. Sci. USA **118**,  
252 e2021203118 (2021), doi:[10.1073/pnas.2021203118](https://doi.org/10.1073/pnas.2021203118).
- 253 [26] D.-X. Qu, Y. S. Hor, J. Xiong, R. J. Cava and N. P. Ong, *Quantum oscillations and Hall*  
254 *anomaly of surface states in the topological insulator Bi<sub>2</sub>Te<sub>3</sub>*, Science **329**, 821 (2010),  
255 doi:[10.1126/science.1189792](https://doi.org/10.1126/science.1189792).
- 256 [27] A. Bharathi, Y. Hariharan, A. Mani and C. S. Sundar, *Positron-lifetime studies in the Kondo*  
257 *insulator FeSi*, Phys. Rev. B **55**, R13385 (1997), doi:[10.1103/PhysRevB.55.R13385](https://doi.org/10.1103/PhysRevB.55.R13385).
- 258 [28] M. Reiner, A. Bauer, M. Leitner, T. Gigl, W. Anwand, M. Butterling, A. Wagner, P. Kudejova,  
259 C. Pfleiderer and C. Huggenschmidt, *Positron spectroscopy of point defects in the skyrmion-*  
260 *lattice compound MnSi*, Sci. Rep. **6**, 29109 (2016), doi:[10.1038/srep29109](https://doi.org/10.1038/srep29109).



- 261 [29] A. Bauer, M. Garst and C. Pfleiderer, *Specific heat of the skyrmion lattice phase*  
262 *and field-induced tricritical point in MnSi*, Phys. Rev. Lett. **110**, 177207 (2013),  
263 doi:[10.1103/PhysRevLett.110.177207](https://doi.org/10.1103/PhysRevLett.110.177207).
- 264 [30] A. Bauer, A. Neubauer, C. Franz, W. Münzer, M. Garst and C. Pfleiderer, *Quantum phase transitions in single-crystal Mn<sub>1-x</sub>Fe<sub>x</sub>Si and Mn<sub>1-x</sub>Co<sub>x</sub>Si: Crystal growth, magnetization, ac susceptibility, and specific heat*, Phys. Rev. B **82**, 064404 (2010),  
265 doi:[10.1103/PhysRevB.82.064404](https://doi.org/10.1103/PhysRevB.82.064404).  
266  
267
- 268 [31] A. Bauer, M. Garst and C. Pfleiderer, *History dependence of the magnetic*  
269 *properties of single-crystal Fe<sub>1-x</sub>Co<sub>x</sub>Si*, Phys. Rev. B **93**, 235144 (2016),  
270 doi:[10.1103/PhysRevB.93.235144](https://doi.org/10.1103/PhysRevB.93.235144).